LA-UR (CONF-8708356--1)

LA-UR--87-3042

DE88 000529

Los Alamos National Laboratory is operated by the University of California for the United States Department of Energy under contract W-7405-ENG-36

TITLE: A REVIEW OF THE EXPERIMENTAL AND THEORETICAL STATUS OF THE REVERSED-FIELD PINCH

AUTHOR(S): D. A. Baker, CTR-DO

SUBMITTED TO: Proceedings of the Energy Independence Conference
Fusion Energy and Plasma Physics
Aug. 17-21, 1987 - Rio de Janeiro, Brazil

DISCLAIMER

MASTER

Los Alamos Los Alamos National Laboratory
Los Alamos, New Mexico 87545

A REVIEW OF THE EXPERIMENTAL AND THEORETICAL STATUS OF THE REVERSED-FIELD PINCH

D. A. BAKER
Los Alamos National Laboratory

ABSTRACT

This paper reviews the status of the reversed-field pinch (RFP) approach to the development of a compact nuclear fusion reactor. Two RFP papers in this conference are complimentary; the first paper[1] contains the historical origins and basic concepts concerning MHD instabilities, relaxation and RFP confinement properties as well as a discussion of future prospects of the RFP. This paper gives an overview of the status of plasma parameters of the present main RFP experiments and of the status of theory and experiment of the interesting RFP plasma phenomena of relaxation, self reversal and flux generation (these effects are often referred to as the dynamo effect). The low frequency oscillating-field current drive concept which exploits these effects is discussed. Particular emphasis is given to the theoretical results obtained from plasma simulation codes used in these active areas of study. Selected topics of recent research on the Los Alamos ZT-40M experiments are reported. The paper concludes with descriptions of the next generation Los Alamos RFP experiment[2] ZTH, to be located in the new Confinement Physics Research Facility[3] (CPRF) presently under construction, and the characteristics of an RFP compact reactor.

I. INTRODUCTION

This paper and companion paper in this conference[1] jointly review the reversed-field pinch (RFP) fusion research concept. The toroidal pinch has a long history which is covered by earlier general review papers[2-5] on the reversed field pinch. The RFP concept has many interesting areas of research both experimentally and theoretically and the authors have of necessity limited their discussion to certain topics. Reference 1 reviews the general origins and basic concepts of the RFP with an emphasis on RFP plasma confinement. It also includes recent results on the ETA-BETA II device, and a description of the new RFX experiment under construction, and comments on future prospects for fusion. The aim of the present paper is to review other topics; these include a short overview of the present RFP experimental devices, an overview of the very recent work in the areas of research on relaxation, flux generation, low frequency current drive, some ZT-40M results, and a general description of the new high-current RFP being designed and constructed at Los Alamos. The paper concludes with a general overview of the RFP compact reactor concept.

II. OVERVIEW OF THE PRESENT RFP EXPERIMENTS

Reversed-field pinch research has recently expanded both in the size and number of experimental devices. Five intermediate sized experiments[6-10] have been in operation for several years and have accumulated extensive databases. A general overview of their characteristics and the published plasma parameters achieved in these devices are summarized in Table I. Plasma temperatures of $\lesssim 0.6$ keV, plasma densities of $\gtrsim 5 \times 10^{20} m^{-3}$ and energy confinement times approaching a millisecond have been obtained. Flat-topped current discharges lasting over 35 msec have been achieved. Most importantly, the plasma temperatures and Lawson $n\tau_E$ products increase with plasma current.[11] This fact has lead to the construction of larger, higher current next generation devices: (1) RFX, a 2MA (R/A = 2 m/0.5 m) experiment under construction in Padova, Italy, in collaboration with the Culham Laboratory in the EURATOM program is discussed in Ref 1.; (2) ZTH, a 4 MA (R/a = 2.4 m/.4 m) experiment, is being constructed at Los Alamos and is discussed in Sec. IV of this paper; and (3) a 2 MA (R/a = 1.5 m/0.25 m) experiment is planned for the near future at the University of Tokyo. There has been an outstanding growth in the number of RFP devices in recent years, particularly in Japan. These are summarized in Table II.

With the above expanded activity in the present and future RFP devices should significantly increase rate of progress in solving outstanding questions in RFP physics.

TABLE I. Range of Parameters for Present Experiments with Large Databases

	TPE-1R(M)	RTA-BETA-II	ZT-40M	OHTE-RFP	HBTX
	ETL (Japan)	PADOVA (Italy)	LOS ALAMOS (United States)	GA TECHNOLOGIES (United States)	CULHAM (United Kingdom)
Major radius, $R_T(m)$	0.5	0.65	1.14	1.24	0.9
Minor radius, $r_p(m)$	0.09	0.125	0.20	0.20	0.26
Peak current, $I_\phi(MA)$	0.15	0.25	0.45	0.80	0.30
Pulse rise time, $\tau_R(ms)$	0.45	0.1 to 0.5	0.25 to 2	0.2 to 0.5	0.3 to 4
Pulse length, $\tau(ms)$	0.8	1.0 to 2.0	5.0 to 37	5.0 to 10	5.0 to 14
$\bar{n}(10^{20}/m^3)$	0.1 to 1.0	0.2 to 4.0	0.1 to 1.0	0.1 to 5.0	0.1 to 1.0
$T_e(0)(eV)$	500 to 600	100 to 200	200 to 400	500	300 to 450
Max. $T_i(eV)$	500 to 600	100 to 200	$\geq T_e(0)$	$\geq T_e(0)$	300 to 450
Poloidal beta, β_θ	~0.1	~0.1	0.1 to 0.2	0.1 to 0.3	0.1 to 0.2
Energy confinement time, $\tau_E(ms)$	~0.1	~0.1	0.3 to 0.7	~0.4	0.1 to ~1.0

TABLE II. RFP EXPERIMENTS

Experiment	Location	R (m)	a (m)	I (kA)	Major Areas of Study
Repute-1	Univ. of Tokyo	0.82	0.2	220.	Equilibrium control with thin shell and feedback
STP-3M	IPP Nagoya Univ.	0.5	0.09	170.	High current density
HIT-1	Hiroshima Univ.	0.25	0.09	100.	Startup and impurity studies
ATRAS	Nikon Univ.	0.5	0.09	--	Start-up
CN-RFP	Nikon Univ.	0.14	(0.38 x 0.1)	10.	Noncircular shape divertors and dynamo
STE-RFP	Kyoto Univ.	0.25	0.1	20.	current drive and divertors
Reversatron	Univ. of Colorado	0.50	0.08	30.	Shell studies
MST	Univ. of Wisconsin	1.4	0.56(ave)	400.	under modification
Multipinch	GA Technologies	--	--	210.	non circular cross-section

III. SOME HIGHLIGHTS OF PRESENT RFP PHYSICS RESEARCH

A. Dynamo Effect - Relaxation-Flux Generation

1. General

One of the most exciting physics topics in RFP research comes from the observed ability of the RFP discharge to maintain its reversed-field configuration in the presence of resistive diffusion. The current is maintained for times well beyond that predicted by classical one dimensional resistive MHD models. A comparison[12] between an actual ZT-40 discharge and classical computation is shown in Fig 1. This ability of the discharge to generate or sustain the toroidal field only by the energy supplied by the toroidal voltage circuit is referred to as the dynamo effect. This is an extension of the use of this term which is identified with the sustainment and generation of fields in the moving and conducting fluids in the earth's core, the sun, and other astrophysical objects. Probably the most striking demonstration of the toroidal field generation occurs during a ramped mode of RFP startup[13] as shown in Fig 2. The net positive toroidal flux increases even though

the toroidal field is negative at the plasma edge as discussed in Ref 12. Positive flux is generated inside the plasma and negative flux is expelled into the external toroidal field circuit.

2. Three-Dimensional MHD Simulations

Several models have been previously proposed to explain the toroidal flux generation and sustainment pinches; see Ref. 4 for references through 1983. Recently extensive studies have been made which examine the process using resistive MHD codes. That three dimensional resistive MHD codes can produce a steady-state reversal mean toroidal field has been demonstrated.[14-17] In an interesting comparison study[16] of five 3-D resistive, time dependent MHD codes, three compressible and two incompressible, it was found that, for the benchmark case tested, the compressible codes produced a steady field reversal while the incompressible codes did not. (See Fig. 3). The study concluded that compressibility is an essential component of the dynamical evolutions of the RFP.

A 3-d pseudospectral computation[17] was made which followed the evolution of an incompressible fluid for a constant applied magnetic field and a hollow non-uniform initial current density. Small scale turbulence develops and the field energy decays faster than the magnetic helicity. The average toroidal magnetic field reverses sign spontaneously. The state that develops is nearly force free, but $\mathbf{J}\cdot\mathbf{B}/B^2$ is not uniform suggesting more residual disorder than that of a pure minimum energy state. These calculations are presently being extended to include compressibility and a driving E field.

The extensive studies with the resistive 3-D MHD codes have indicated the following:

1. The maintenance of toroidal field reversal by the nonlinear evolution of $n = 1$ resistive modes.
2. The nonlinear interaction of many $n = 1$ modes can lead to a stochastic core with good surfaces outside for low $\theta < 1.6$.
3. Long time oscillatory behavior occurs at high theta.
4. Unlike for the tokamak description, when many resistive tearing modes interact and cause disruption, for the RFP the driven modes remain stable and have a stabilizing effect on the dominant growing modes.[18]

The Result 2 above suggests that for normal low theta operation the confinement of the RFP may be sensitively effected by the plasma edge properties, field errors, limiters, etc. Plasma edge physics has become a very active RFP research area.[19-23]

There are limitations on 3-D codes due to boundary conditions that are used,[24] finite resolution (mesh size and mode truncation), practical running time, and upper limits on the practical Lundquist number (resistive diffusion time/Alfvén time) thus leaving plenty of room for more work to achieve significant improvements in the future.

3. Reduced MHD Equations

Reduced MHD equations[25] for the mean and fluctuating fields have been derived and applied to the RFP. These approximate equations are used to analyze the mean and fluctuating fields and produce equations easily solved numerically. Solutions to these equations indeed produce self reversal as shown also in Fig. 4. The reduced equations have been used to show that quasilinear treatment of growing and stationary tearing modes can be calculated and are consistent with field reversal in the RFP.

4. Sawtooth Activity

At high values of the pinch parameter $\theta = B_{pol}(a)/B_{\phi ave}$, large sawtooth oscillations are seen on ZT-40. In contrast to the relatively smooth sustainment of the toroidal flux at low theta values, in this case the dynamo acts to restore the flux in discrete jumps[26] for high theta operation. These observable events have been studied in detail[27] and it was found that a one dimensional transport description was sufficient to model the risetime portion of the sawtooth if the resistivity profile is not flat, but instead has resistivity gradients located at less than half the plasma radius. These studies resulted in the following picture: The sawtooth starts at state of minimum energy and evolves away from that state by ohmic heating which peaks the current on axis driving the system into instability. These instabilities enter a nonlinear phase causing the sawtooth crash returning the plasma to the previous minimum energy state and the process repeats. Studies of the stability of these profiles during the ohmic heating phase indicate that the crash and flux generation are produced by current-driven tearing modes. Experimentally large scale m = 1, n $\simeq$ 8-15 modes have been associated with the crash.[27]

5. Current Ramping Simulation

Dynamo action during Current Ramping startup has been recently examined[28] with a 3-D MHD code with the conclusion that this mode of RFP operation, in which the toroidal flux generation is the most pronounced, can be simulated. The long-wavelength and low frequency tearing instabilities are sufficient to give the observed flux generation and the strong nonlinear coupling observed between the toroidal and poloidal field circuits. It is acknowledged, however, that the calculated edge field fluctuations are larger than observed experimentally. This is one of the main discrepancies between the numerical MHD predictions of the dynamo action and experiment for both ramped and steady current operation. An important question in this regard is whether the inclusion of a large number of modes, i.e., fine spatial and temporal resolution and the use of the high experimental Lundquist numbers, would allow resistive MHD to predict the low level turbulence observed in the low theta RFP discharges. This question remains open as a result of the limitations on present day computers.

B. ANALYTIC WORK ON RELAXATION

Since this area of research is reviewed in Ref. 1, only a few comments on recent work are given here. Work continues along several approaches to further study the effects of relaxation and flux generation. The results of an early statistical study of the RFP state[29] has been followed[30] by a deterministic approach for incompressible dissipative MHD. The reversed field state was shown to be a quasi-steady state that is stable as an attractor.

A recent calculation minimizing energy, with constraints on magnetic helicity, hybrid helicity, axial magnetic flux, and fluid velocity flux, gives a relaxed state which is not force free.[31]

A study has been made of the radial distribution of the dynamo mean electric field needed to sustain steady-state cylindrical RFP when prescribed values of $\lambda(r) = \mathbf{J} \cdot \mathbf{B}/B^2$ and thermal transport functions are given.[32] It was found that: (1) energy was extracted from the central core to drive the poloidal large currents of the RFP configuration; (2) the quantitative results are only weakly dependent on the choice of parameters; and (3) comparisons with experiments indicate that the resistance of the plasma may not be far from classical. Conclusion (1) agrees with past work on the kinetic dynamo model in which electrons pick up energy in the core and then are transported across a postulated ergodic field line region to produce the currents for the reversed field in the outer region.[33] Conclusion (2) also agrees with earlier work in which the plasma resistivity is estimated using magnetic helicity.[34]

A new dynamo model has appeared very recently.[35] It is a spin off from the Rotamak concept in which current drive is produced by rotating fields in a regime where the Hall term in ohms law dominates the resistive term and the electrons are frozen to the magnetic field while the ions are not. The proposed mechanism uses a non-linear Hall effect of a saturated helical mode. Preliminary calculations predict the correct direction and magnitude for the poloidal current density that was observed in HBTX1A. The observed small magnetic field fluctuation ~2% level is reported to be sufficient to give agreement with the experiment.

C. CURRENT DRIVE

The advantages of steady state reactors over pulsed ones have motivated studies both experimentally and theoretically for driving tokamaks, including particle beam injection and various radio-frequency drive schemes. These techniques seek to avoid the continuous increase of poloidal flux that threads the hole in the torus for normal inductive drive. There is an equivalent need for such a system for the toroidal RFP. In addition to the methods available to the tokamaks, there is also the possibility of a method[36] which uses a low (audio) frequency ac modulation of the toroidal and poloidal field to produce a unidirectional current. This method, if successful, would replace expensive r.f. or particle beam equipment with low cost ac power supplies. The technique was first explored using 0-D models.[37,38] Using the assumption of instantaneous relaxation to a preferred state

and energy balance in the form of the Poynting theorem, one obtains an equation for the toroidal loop voltage[37]

$$V_\phi = I_\phi R_p + F_1(\theta)\dot{I}_\phi + F_2(\theta)V_\theta \ , \tag{1}$$

where I_ϕ is the toroidal current, $R_p = I_\phi^{-2}\int \mathbf{J}\cdot\mathbf{E}dV$ (the integral extends over the plasma volume), V_θ is the poloidal voltage and $F_1(\theta)$ and $F_2(\theta)$ are functions of the pinch parameter θ. The precise form of these functions depends on the magnetic field profiles.[37] When a small signal analysis is used and assuming the changes in R_p are negligible, the direct current component for steady state has the form[37,39]

$$I_{dc} = \frac{K\hat{V}_\phi\hat{V}_\theta \sin\delta}{2w\langle\phi\rangle R_p} \ , \tag{2}$$

where the modulating voltages are given by $V_\theta = \hat{V}_\theta \sin wt$, $V_\phi = \hat{V}_\phi \sin(wt-\delta)$, and $\langle\phi\rangle$ is the mean toroidal flux. The coefficient K depends on the mean-field profiles. This expression is maximum when the phase angle δ is 90°. Alternatively, one may integrate equation (1) directly allowing one to drop the mathematical restriction that the modulating voltages be small. A sample solution obtained by integrating Eq. (1) using the Modified Bessel Function model[40] is shown in Fig. 5. Critical to the system is the value of the effective plasma resistance, R_p, because it determines whether current drive can be obtained for practical values of the amplitude of the oscillating voltages. Since the resistivity should drop in the next generation high current, high temperature experiments (and even more in reactor level plasma), the required driving amplitude on the oscillating voltages will be reduced. Studies of the effects of varying phase of modulations impressed on normally inductively driven flat top discharges in ZT-40M have been made.[41] The arrangement for driving the field windings is shown schematically in Fig. 6. Waveforms for optimum phase $\delta = \pi/2$ (called pumping) $\delta = \pi$ (called dumping, which drives a reverse component of current) are shown along with an unmodulated current in Fig. 7. The agreement in the trends observed in 0-D simulation is encouraging, indicating that this plasma is responding in the correct way to give current drive. The fact that the current did not actually increase in the pumping case in Fig. 7 is evidently due to an enhanced resistance due to plasma-wall interactions accompanying the modulations. It is noted that the amount of modulation on V_θ is limited if the reversed toroidal field is retained. Loss of field reversal is known to dramatically raise the plasma resistance. Somewhat improved behavior has been obtained when the modulations were applied during a ramp[43] so that the mean Poynting vector was directed radially inward.

Recently, 1-D calculations have been made using MHD codes to examine the details of the plasma response during oscillating field-current drive.[44,45] Since the MHD relaxation is basically three dimensional, some means for modelling the relaxation needs to be included in the 1-D calculations. One approach is to periodically force the field profiles to relax.[46] Another approach modifies Ohm's law in the 1-D MHD codes by adding an α effect term[47]

$$\mathbf{E} = \eta\mathbf{J} + \mathbf{v}\times\mathbf{B} + \alpha\mathbf{B} \ . \tag{3}$$

An expression for the α coefficient of the form

$$\alpha = B^{-2}\nabla\cdot\left[B^2 D\nabla\mathbf{J}\cdot\mathbf{B}/B^2\right] \tag{4}$$

has been discussed by several authors.[48-50] D is a coefficient which controls the flattening of the λ profile. The spatial variation of D must be specified, e.g., from 3-D code results or from a theory. The hyper-resistivity term (4) allows one and two dimensional codes and to be able to produce the RFP profiles[45,48] and to generate toroidal flux during 2-D ramped current simulations.[51] This expression for α has also been shown, under certain assumptions, to conserve magnetic helicity while dissipating energy.[52] The 1-D simulations have been successful in demonstrating current drive without flux consumption. It has been shown that $m = 1$ helical perturbations are needed for the resistive MHD model to give oscillating field current drive. A class of $m = 1$ tearing modes which can generate the required poloidal flux have been identified[45,52] and are driven unstable by the development of an off-axis peak in the λ profile.[53]

This area of research is currently very active both theoretically and experimentally in order to determine both the physics properties and engineering requirements for this approach to current drive.

D. FUELING AND DENSITY CONTROL

Experiments[42,54,55] have been carried out using injection of solid fueling pellets into reverse field pinch discharges. In ZT-40M a four barrel pneumatic pellet injector previously used on Alcator C.[50] Injection was along a major radius and resulted in as high as a factor of six increase in density. A characteristic behavior was a deflection of the pellet both toroidally and poloidally upon entering the discharge. This effect is interpreted as produced by an asymmetric ablation of the pellet by impact with electron currents flowing along the magnetic field. This effect will be useful as a diagnostic for RFP plasmas.

It is observed that when neutral gas injection is used concurrently with pellet injection, the effectiveness of both is increased. This effect may be due to an increased neutral density at the plasma edge from the gas puffing, which suppresses the energetic electrons causing the asymmetric ablation as the pellet enters the discharge region.

The results to date have demonstrated the ability to increase and sustain the density in an RFP. This technique appears to be a viable method of density control needed in the future long-pulse high-current devices.

IV. THE ZTH EXPERIMENT

A next generation RFP experiment ZTH will be the initial experiment in the new confinement physics research facility (CPRF) under construction at Los Alamos.[57,58]

The experiment will be located in an existing building having thick concrete walls and ceiling to give adequate neutron shielding for the projected plasma parameters. The experiment will be powered by a 1,430 MVA, 600 MJ generator operating over the frequency range of 60 to 42 Hz. Power conversion equipment will drive up to 4 MA plasma current

into the ZTH experiment. The generator can be fitted with a flywheel which will provide 1,400 MJ of additional energy. Key design quantities of the experiment and projected plasma parameters for ZTH are given in Table 3.

TABLE 3. ZTH DESIGN SPECIFICATIONS

Symbol	Quantity	Design Value	Comments
R	Major Radius (liner)	2.4 m	
a	Minor Radius (liner)	0.4 m	
R/a	Aspect Ratio	6.m	
I_ϕ	Max. Toroidal Current	4 MA	Range: 0.5 to 4
τ_r	I_ϕ Rise Time	50ms	
β_p	poloidal beta	0.1	Range: 0 to 0.2
ℓ_i	Shafranov Int. Inductance	1.4	Range: 0.5 to 2
τ_s	Shell Time Constant	$\sim$ 50ms	
R_e	Liner resistance	8.5 mΩ	
V_ϕ	Toroidal voltage	7V	20 V @ 0.5 MA
$V \cdot s$	volt seconds	28.8	For 60 MA in OH Coil
	Projected Plasma Quantities at 4 MA[57]		
T	Temperature $T_e \approx T_i$	$\sim$4 keV	
$\bar{n}_e$	Electron density	$\sim 2.5 \times 10^{20} m^{-3}$	
τ_E	Energy containment time	$\sim$85 ms	

An artist's conception of the ZTH device is shown in Fig. 7 and a cross-section layout is shown in Fig. 8. The coil arrangement is shown in Fig. 9.

The design of ZTH has the following objectives for the first phase:

1. Optimize the formation, current ramping, and plasma equilibrium control.

2. Determine the suitability of graphite armor for wall protection at high wall loading

3. Determine scaling properties of plasma parameters (beta, density, and temperature) as I_ϕ is increased up to 4 MA.

4. Explore methods of ramp down with gradual current termination.

The second phase of the experiments will require some system modification and will be used to explore the following:

1. Optimization of density control with pellet injection, gas puffing, etc.

2. Impurity control and divertors.

3. Explore the oscillating field current drive and other schemes as dictated by the results.

The new experiment is scheduled to begin operation with plasma current capability of 2 MA in May 1991 and with a 4 MA capability in September 1992.

V. THE REVERSED-FIELD PINCH AS A COMPACT REACTOR

One of the characteristic features of the reversed-field pinch is that it allows a high engineering beta (plasma pressure/field pressure at the coils), a feature which results from the fact that the main poloidal confining field is supplied by the plasma and drops to lower values outside the plasma. This property has allowed the development of the concept of a small, high power density compact fusion reactor[59,60] using resistive coils and thin blankets as an alternative to the earlier large, low power density designs[61] utilizing thick blankets and super-conducting coils. The advisability of such a change in direction in reactor designs is suggested by studies[62,63] which indicate that the cost of electricity from the large fusion reactors project to be 50–100% above the alternative nuclear energy sources. The smaller compact designs are able to project lower electricity costs because the cost of the fusion power core (the plasma chamber, first wall, blanket, shield, magnets, and structure) contributes a significant fraction to the price of the electricity. This cost increases with the amount of material in the fusion power core, and studies[64,65] have concluded that the ratio of net electric power to fusion power core mass (mass power density) should be 100-120 kWe/tonne or more to be competitive with the cost of electricity from pressurized water fission reactors. Framework studies[66,67] of the RFP compact reactor project designs with mass power densities of > 3 MWe/tonne, more than an order of magnitude improvement over the value for the conventional large fusion reactor designs.

The RFP has other distinctive features which promise attractive reactor properties. It operates successfully at high current densities, is not bound by the Kruskal limiting current, allows designs which utilize simple ohmic heating to ignition, and puts no constraints on the toroidal aspect ratio. The plasma relaxation to a preferred state gives a strong coupling between the poloidal and toroidal field circuits; this gives promise for a steady state current drive using low frequency fields as described earlier. A sample set of design parameters and characteristics from Ref. 67 CRFPR (20) are given in Table 4. A layout of the fusion power core is shown Fig. 9 and a sample plant layout for this design is shown in Fig. 10. Optimization studies and other arrangements are given in Ref. 67.

Further detailed studies of the RFP fusion reactor are currently being undertaken by a multi-institutional TITAN program, and the results of a first step scoping study are available.[68] This scoping study explored a large number of design options, and confirmed that the RFP concept system with high power densitites and with neutron wall loadings

TABLE IV. Key CRFPR Engineering Parameters and Characteristics for the $I_w = 19.5\ MW/m^3$, CRFPR(20) Design from Ref. 67.

Net/Gross electric power, $P_E[MW(electric)]/E_{ET}[MW(electric)]$	1,000/1,256
Total thermal power, $P_{TH}[MW(thermal)]$	3,473
Gross power-conversion efficiency, η_{TH}	0.369
Recirculation power fraction, ϵ	0.204
Overall plant availability, p_f	0.75 (15 MW · yr/m^2 FPC life)
Major/minor plasma radius, R_T/r_p (m)	3.9/0.71
Plasma volume, V_p (m^3)	38.8
First-wall area, $A_{FW}(M^2)$	115
Neutron first-wall loading, $I_w(MW/m^2)$	19.0
Number of toroidal section, N	24[a]
Maximum field at magnet, $B_{\theta c}(T)$	4.5[b]
Field at plasma axis/edge, $B_\phi(0)/B_\theta(r_p)(T)$	9.5/5.2
Average poloidal/total beta, β_θ/β	0.23/0.12
Average D-T ion density/temperature $n(10^{20}/m^3)/T(keV)$	6.6/16.0
Plasma burn mode	Continuous/ignited[c]
Plasma heating method (startup)	Ohmic (246 $V \cdot s$ total, 26 $V \cdot s$, ohmic)
Plasma current/ohmic power (MA/MW)	18.4/25.3
Plasma impurity control method	Poloidal pumped limiter (24, 38% first wall)
First-wall/limiter materials	MZC copper alloy (water cooled)
Blanket/shield structural material	HT-9 steel (water-cooled second wall)
Tritium-breeding medium	Li-Pb (35 MW/m^3 average), tritium breeding ratio = 1.06 (two dimensional)
Primary coolant	Li-Pb (poloidal flow, 0.6 m thick)
Shield	Stainless Steel (0.1 m thick, water cooled)
Thermal-conversion method	Dual-medium (~40% H_2O, ~60% Li-Pb) steam
Total Fusion Power Core Weight	1,117 tonnes

(*a*) For off-site fabrication purposes only, single-piece or batch FPC maintenance is envisaged for this system that weighs ~305 tonnes (first wall, blanket, shield, TFCs), to which is added a separate 813-tonne PFC set and ~943 tonnes of Li-Pb coolant.

(*b*) At the OHC during the burn, 9.2 T during startup. Peak field at the TFC is 6.7 T, with the plasma dynamo providing a major part of the toroidal flux during startup. The TFC/OHC/EFC power consumption is 12.6/73.0/53.5 MW (electric), with the OHC power going to zero upon initiation of $F - \Theta$ pumping current drive.

(*c*) Based on $F - \Theta$ pumping at 50 Hz with $\delta\Phi/\Phi \sim 0.035$ toroidal flux swing, $\delta I_\phi/(I_\phi f_A R_p) \sim 100$, $\delta I_\phi/I_\phi \sim 0.01$ plasma current swing.

in the range 15-20 MW/m^2 can have a fusion power core whose cost would be less than 10% of the total plant cost. This means that small units can be used to minimize the cost of a development program. The design phase of the TITAN program is in progress and is expected to lead to further advancement toward the goal of an attractive RFP fusion reactor.

ACKNOWLEDGEMENTS

The author acknowledges the RFP community whose publications have been utilized in the paper. Particular thanks are due to my colleagues on the Los Alamos RFP Team.

REFERENCES

1. S. Ortolani, "Plasma Confinement in Reversed-Field Pinches," Paper 13R-8, this conference.

2. H. A. B. Bodin and A. A. Newton, Nucl. Fusion, 20, 1255 (1980).

3. D. A. Baker and W. B. Quinn, Fusion, 1, Part A, Chap. 7, E. Teller, Editor, Academic Press, Inc., New York, NY (1981).

4. D. A. Baker, AGU Geophysical Monograph, 30, E. W. Hones, Jr., editor, (American Geophysical Union, Wash, DC, 1984), p. 332.

5. H. A. B. Bodin, R. A. K. akowski, and S. Ortolani, "The Reversed Field Pinch: From Experiment to Reactor," Fusion Tech., 10, 307 (November 1986).

6. T. Shimada, Y. Hirano, Y. Yagi, A. A. Newton, and K. Ogawa, 11th Int. Conf. on Plasma Physics and Controlled Nuclear Fusion Research, Kyoto, Japan, paper IAEA-CN-47 (1986), IAEA, Vienna, Austria.

7. V. Antoni, et al., 10th Int. Conf. on Plasma Physics and Controlled Nuclear Fusion Research, London, England, 2, 487, IAEA, Vienna, Austria (1985).

8. D. A. Baker, et al., 10th Int. Conf. on Plasma Physics and Controlled Nuclear Fusion Research, London, England, 2, 439, IAEA, Vienna, Austria (1985).

9. T. Tamono, W. D. Bard, T. N. Calstrom, Proc. 10th Int. Conf. on Plasma Physics and Controlled Nuclear Fusion Research, London, 2, 431 (1985).

10. B. Alper, et al., Proc. 11th Int. Conf. on Plasma Physics and Controlled Nuclear Fusion Research, Kyoto, Japan, paper IAEA-CN-47 (1986), IAEA, Vienna, Austria.

11. R. S. Massey, R. S. Watt, P. G.Weber, G. A. Wurden, et al., Fusion Tech. 8, 1571 (1985).

12. E. J. Caramana and D. A. Baker, Nucl. Fusion 24, 423 (1984).

13. J. A. Phillips, et al., "Observations of Ramped Current Operation in ZT-40M," Los Alamos National Laboratory report LA-10060-MS (1984).

14. A. Sykes and J. A. Wesson, in Proc. 8th European Conf. on Controlled Fusion and Plasma Physics, (Czechoslovakia Academy of Sciences, Prague, 1977) p. 80.

15. A. Y. Aydemir and D. C. Barnes, Phys. Rev. Lett. 52, 930 (1984).

16. A. Y. Aydimir, D. C. Barnes, E. J. Caramana, A. A. Mirin, R. A. Nebel, Phys. Fluids 28, 898 (1985).

17. J. P. Dahlburg, D. Montgomery, G D. Doulen, and L. Turner, J. Plasma Phys. 37, 989 (1985).

18. J. A. Holmes, B. A. Caneras, T. C. Hender, H. R. Hicks, and V. E. Lynch, Phys. Fluids 28, 261 (1985).

19. J. Weiland, J. P. Mondt, Phys. Fluids, 28, 1816 (1985).

20. J. Weiland, J. P. Mondt, Phys. Fluids, 28, 1735 (1985).

21. R. B. Howell, J. C. Ingraham, G. A. Wurden, P. G. Weber, and C. J. Buchenauer, Phys. Fluids, 30, 1828 (1987).

22. T. R. Jarboe and B. Alper, Phys. Fluids, 30, 1177 (1987).

23. H. Y. W. Tsui, 14th Conf. on Controlled Fusion and Plasma Physics, Madrid, June 22-26 (1987).

24. A. A. Mirin, Phys. Fluids, 29, 3018 (1986).

25. H. R. Strauss, Phys. Fluids, 28, 2786 (1985).

26. R. G. Watt and R. A. Nebel, Phys. Fluids, 26, 1168 (1983).

27. K. A. Werley, R. A. Nebel, and G. A. Wurden, Phys. Fluids, 28, 1450 (1985).

28. E. J. Caramana and D. D. Schnack, Phys. Fluids 29, 3023 (1986).

47. H. G. Moffatt, "Magnetic Field Generation in Electrically Conducting Fluids," Cambridge University, MA (1978).

48. H. R. Strauss, Phys. Fluids 28, 2786 (1985).

49. A. Battachariee, E. Hameiri, Phys. Rev. Lett. 57, 206 (1986).

50. A. Boozer, J. Plasma Physics 35, 133 (1986).

51. D. A. Baker, K. M. Ling, S. C. Jardin, N. Pomphrey, Sherwood Theory Conference, April 6–8, San Diego, CA, p. 341 (1987).

52. R. A. Scardovelli, Ph. D. thesis, University of Illinois, Urbana, IL (1987).

53. E.J. Caramana, R. A. Nebel, and D. D. Schnack, Phys. Fluids 26, 1305 (1983).

54. G. A. Wurden, P. G. Weber, R. G. Watt, et al., Nuc. Fusion 27, 857 (1987).

55. B. Alper, V. Antoni, et al., Proc. 11th Int. Conf. on Plasma Physics and Controlled Nuclear Fusion Research, paper IAEA-CN-47/D-11-3, Kyoto, Japan (1986) IAEA Vienna.

56. M. Greenwald, et al., Phys. Rev. Lett. 53, 352 (1984).

57. P. Thullen and K. F. Schoenberg, editors, ZTH Reversed field Pinch Experiment Technical Proposal, Los Alamos National Laboratory report LA-UR-84-2502, (1984).

58. P. Thullen, compiler, CPRF Specification, Los Alamos National Laboratory report LA-UR-85-3338, (1985).

59. R. A. Krakowski and R. L. Hagenson, Nucl. Tech. Fusion 4, 1265 (1983).

60. R. A. Krakowski, R. L. Hagenson, and R. L. Miller, Proc. 13th Symposium on Fusion Tech., Varese, Italy (Sept. 24-28, 1984).

61. R. Hancox, R. A. Krakowski, and W. R. Spears, Nucl. Eng. Des. 63, 2, 251 (1981).

62. C. C. Baker and M. A. Abdou, Argonne National Laboratory report ANL/FPP-80-A (1980).

63. B. G. Logan, C. D. Henning, G. A. Carlson, R. W. Werner, D. E. Baldwin, W. L. Barr, et al.,

64. R. W. Conn, (editor), "Panel X Report to the Magnetic Advisory Committee (May 8, 1985).

65. J. Sheffield, R. A. Dory, S. M. Cohn, J. G. Delene, and L. Parsley, Fus. Tech. 9 199 (1986).

66. R. L. Hagenson, R. A. Krakowski, C. G. Bathke, R. L. Miller, M. J. Embrechts, N. M. Schnurr, M. E. Battat, R. S. LaBauve, and J. W. Wiley, Los Alamos National Laboratory report, LA-10200-MS (1984).

67. C. Copenhaver, R. A. Krakowski, N. M. Schnurr, R. L. Miller, C. G. Bathke, R. L. Hagenson, et al., Los alamos National Laboratory report LA-10500-MS (1985).

68. F. Najmabadi, N. M. Ghoniem, R. W. Conn, et al., "The Titan Reversed-Field Pinch Fusion Reactor Study," Report UCLA-PPG-1100 (1987).

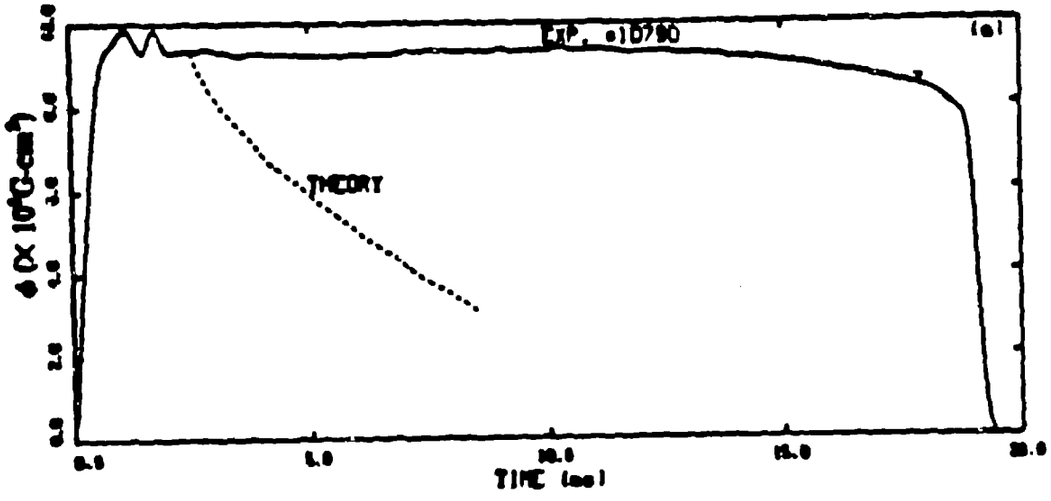

Fig. 1. Comparison of the toroidal flux in ZT-40M with a one-dimensional computer code using the measured toroidal voltage and fieldline pitch as boundary conditions. The sustainment of the flux by the dynamo action is evident.[12]

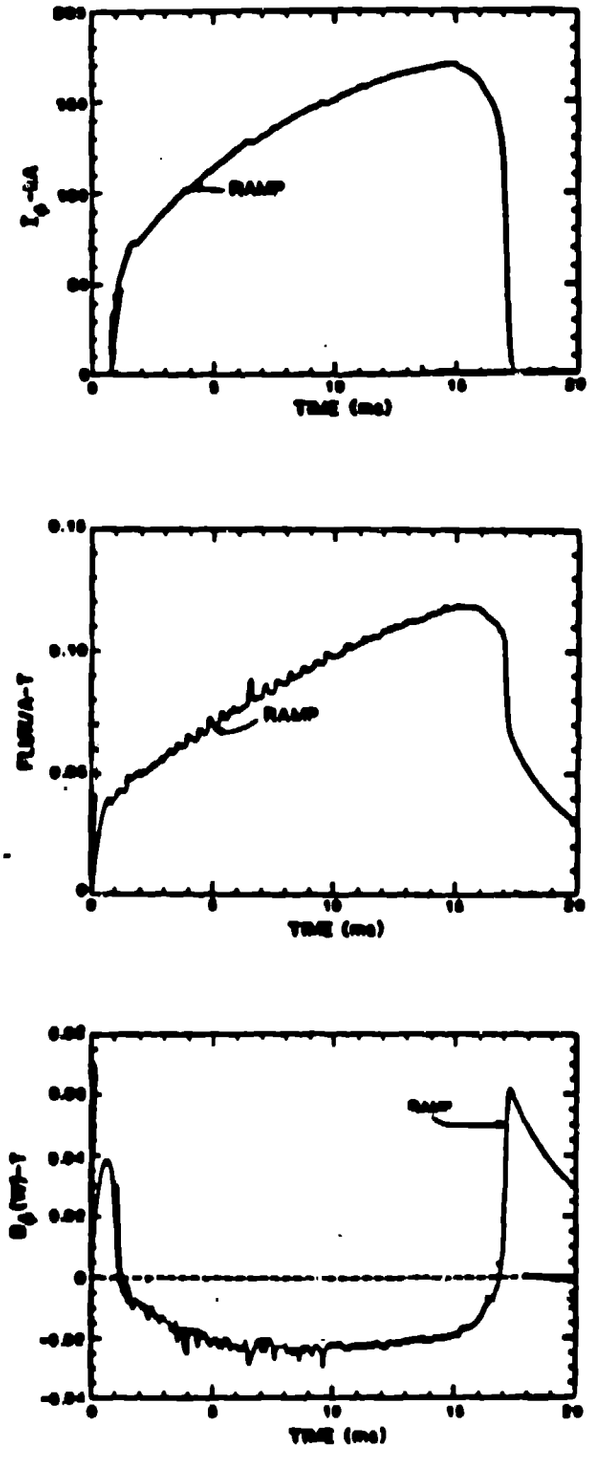

Fig. 2. Ramped mode of operation when a toroidal field increased by dynamo throughout the ramped part of the rise.[13]

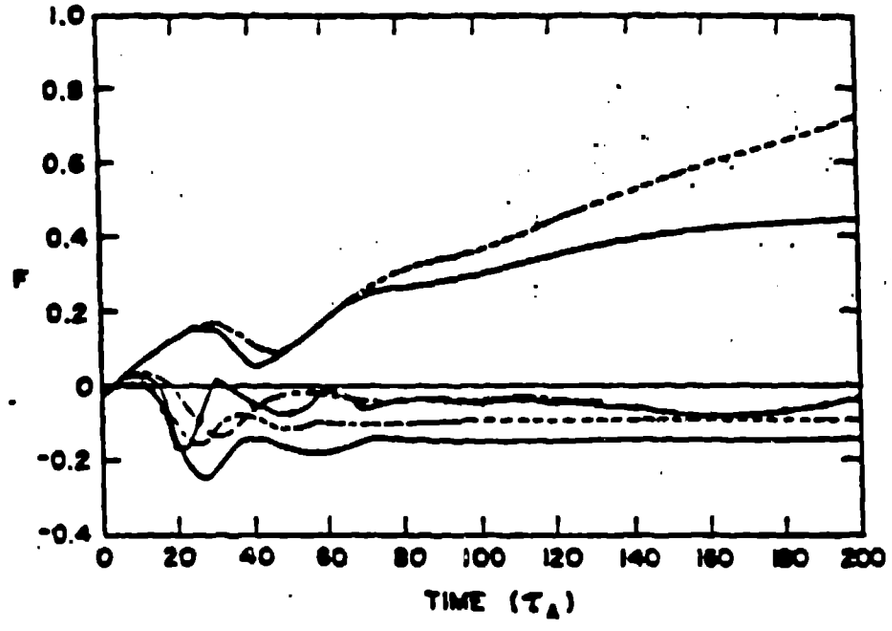

Fig. 3. Reversal factor F *versus* time. Upper two curves are the incompressible results. Four lower curves are the compressible cases.[16,38]

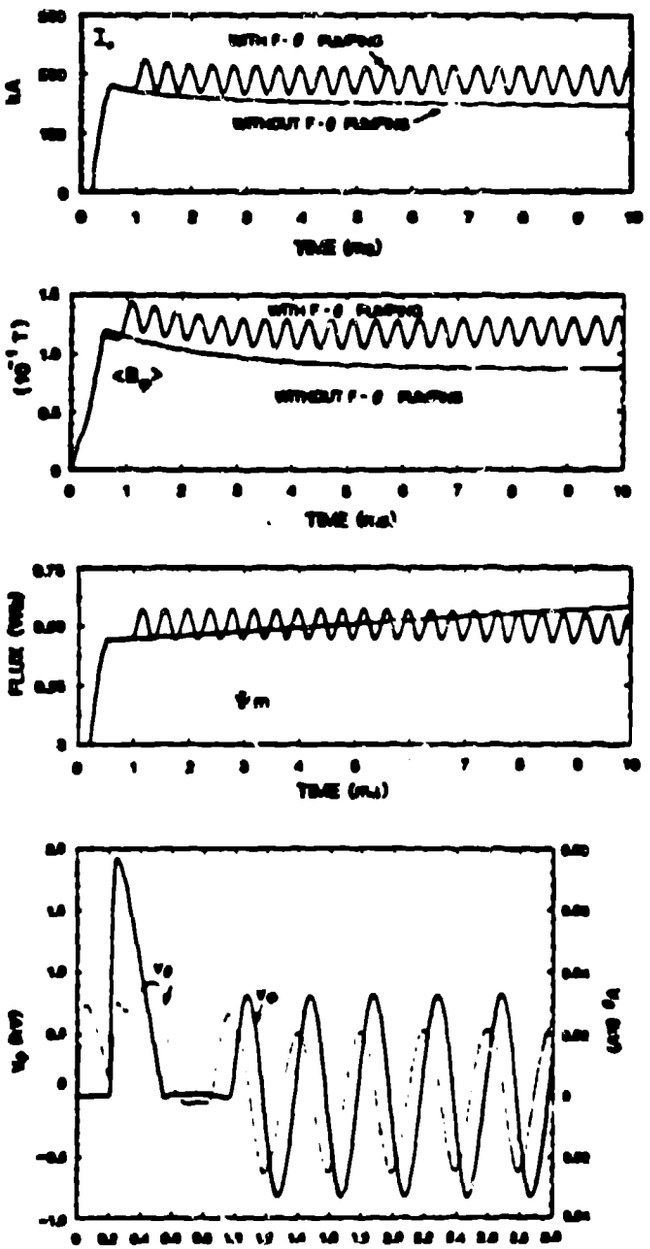

Fig. 4. Computational simulations of $F-\Theta$ pumping on ZT-40M. (a) Plasma current with and without $F-\Theta$ pumping. (b) Mean toroidal field with and without $F-\Theta$ pumping. (c) Simulated waveform for the magnetizing flux (Ψ_m) during $F-\Theta$ pumping. Here, Ψ_m dontes the magnetic flux threading the central hole of the torus. (d) Applied voltages V_θ and V_ϕ at the plasma.[37]

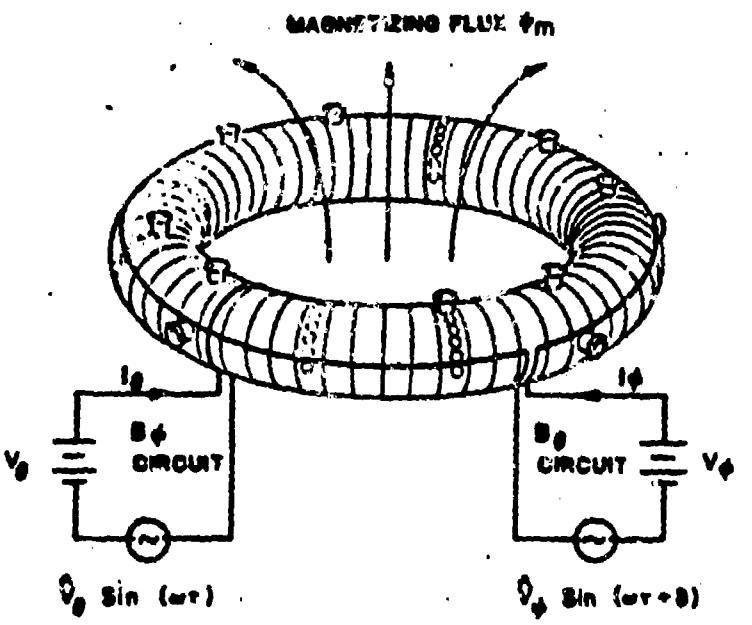

Fig. 5. Oscillating field current drive schematic.[37]

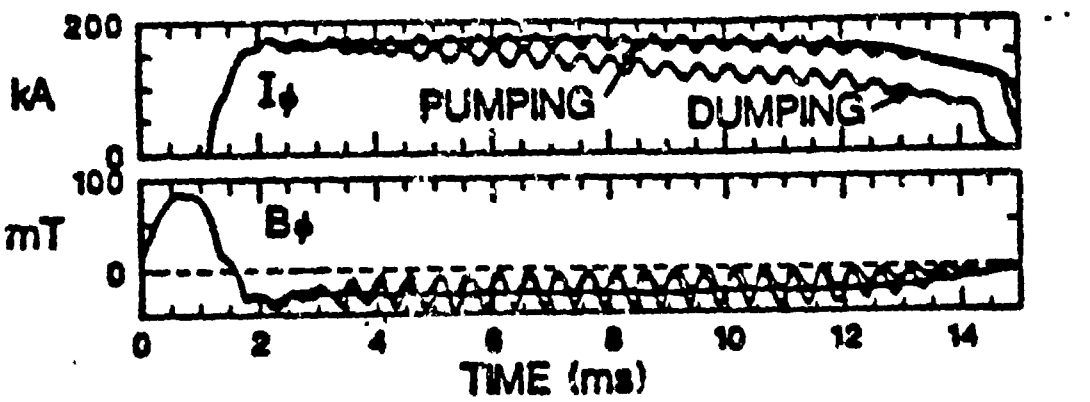

Fig. 6. Plasma current (I_ϕ) and toroidal magnetic field at the plasma edge [$B_\phi(a)$] for one non-modulated and two OFCD discharges.[42]

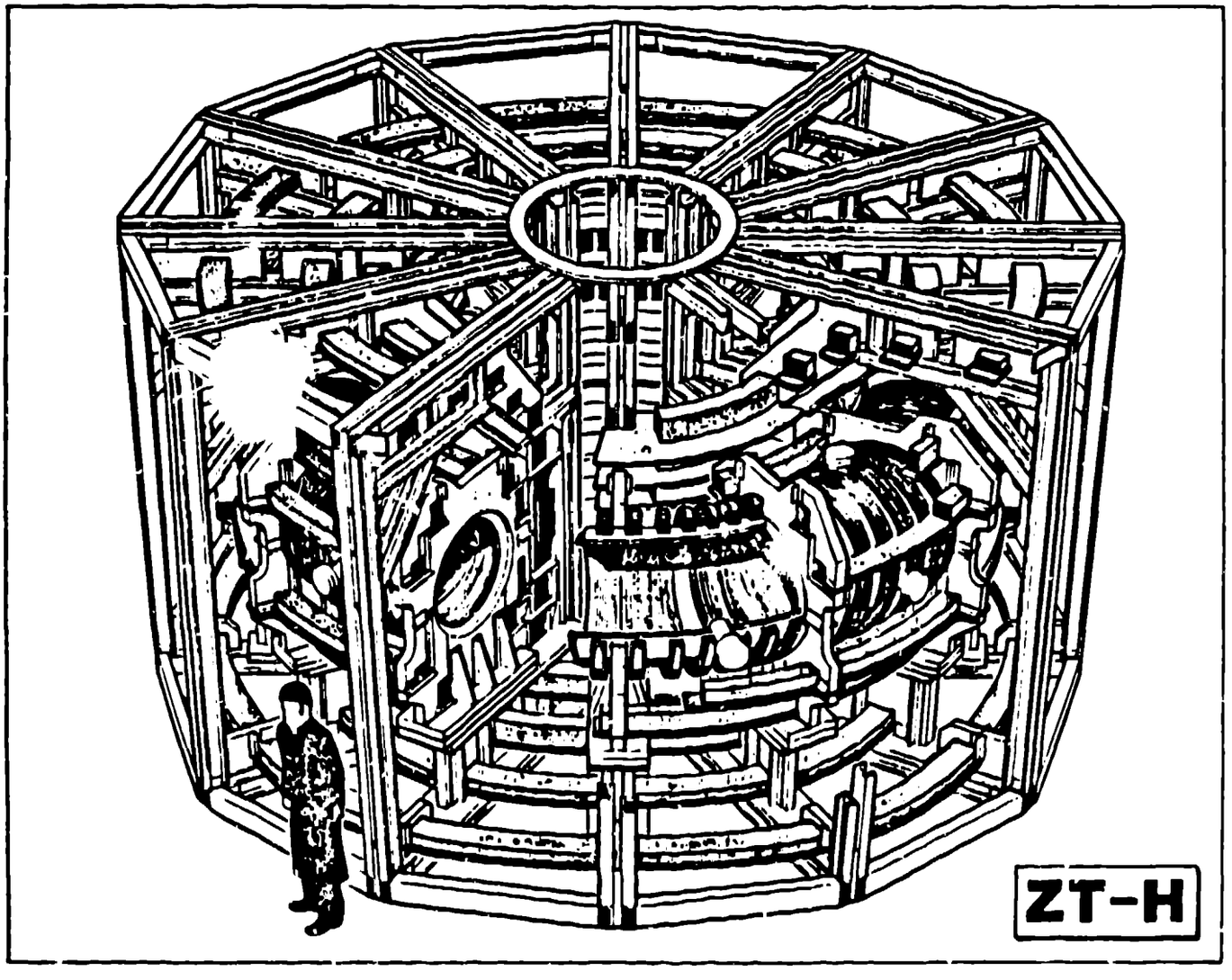

Fig. 7.

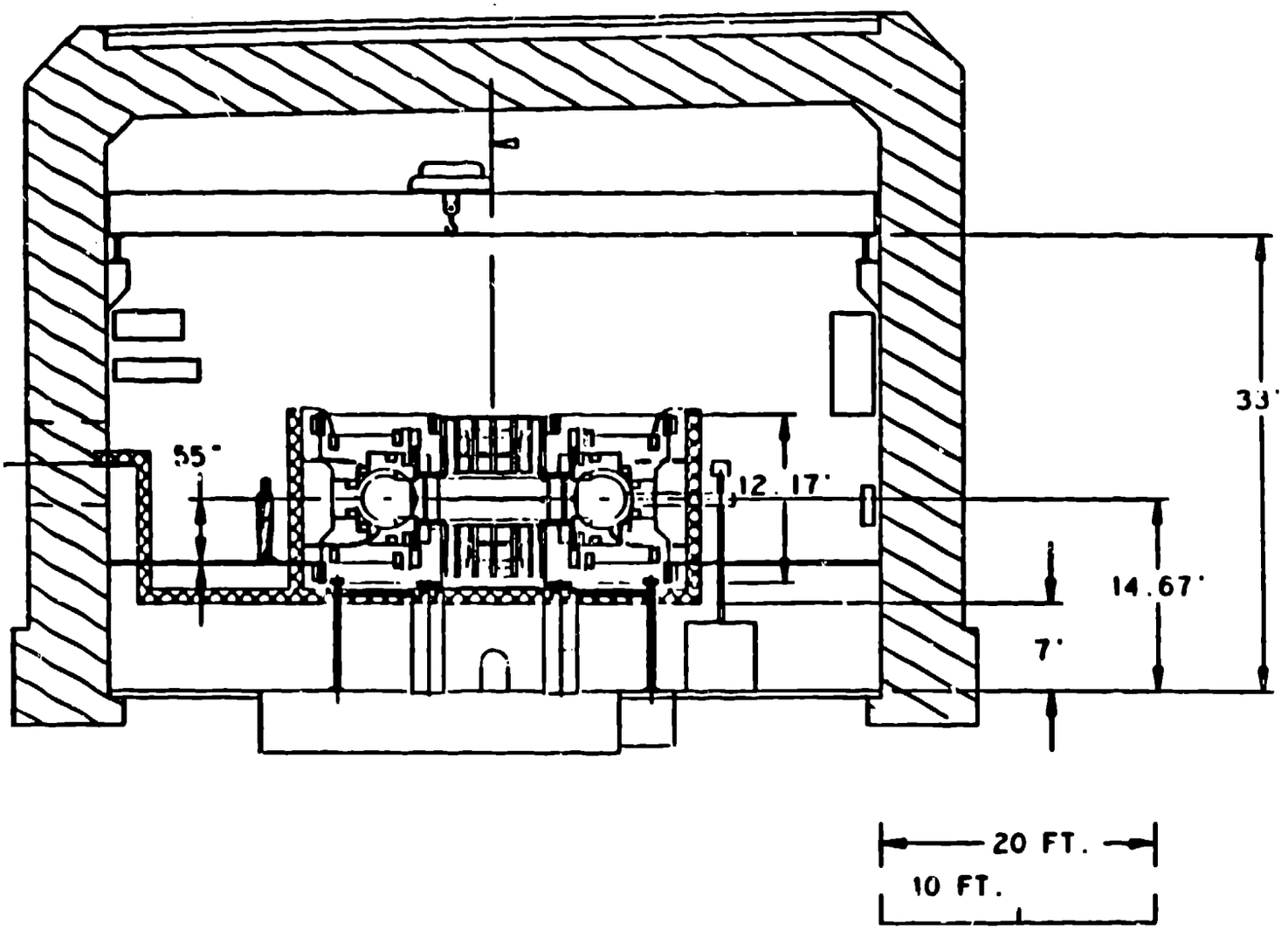

Fig. 8. Cross-section view of TSL 124 and ZTH.

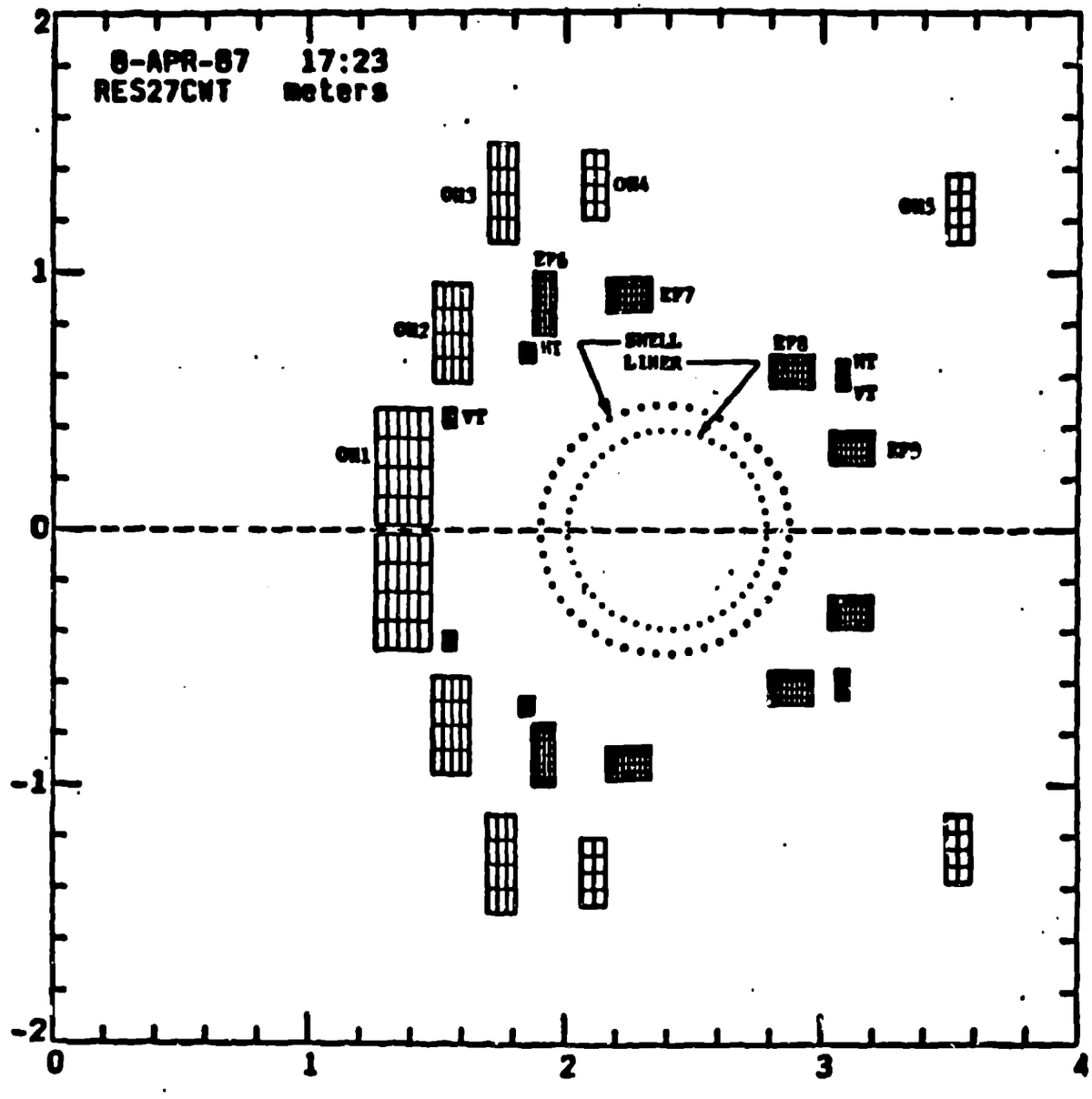

Fig. 9. Optimized coil configuration for ZTII, OII, EF, HT, and VT distinguish the ohmic heating, equilibrium horizontal trim and the vertical trim coils respectively. Shown also are the loops used to model the shell, liner, and plasma.

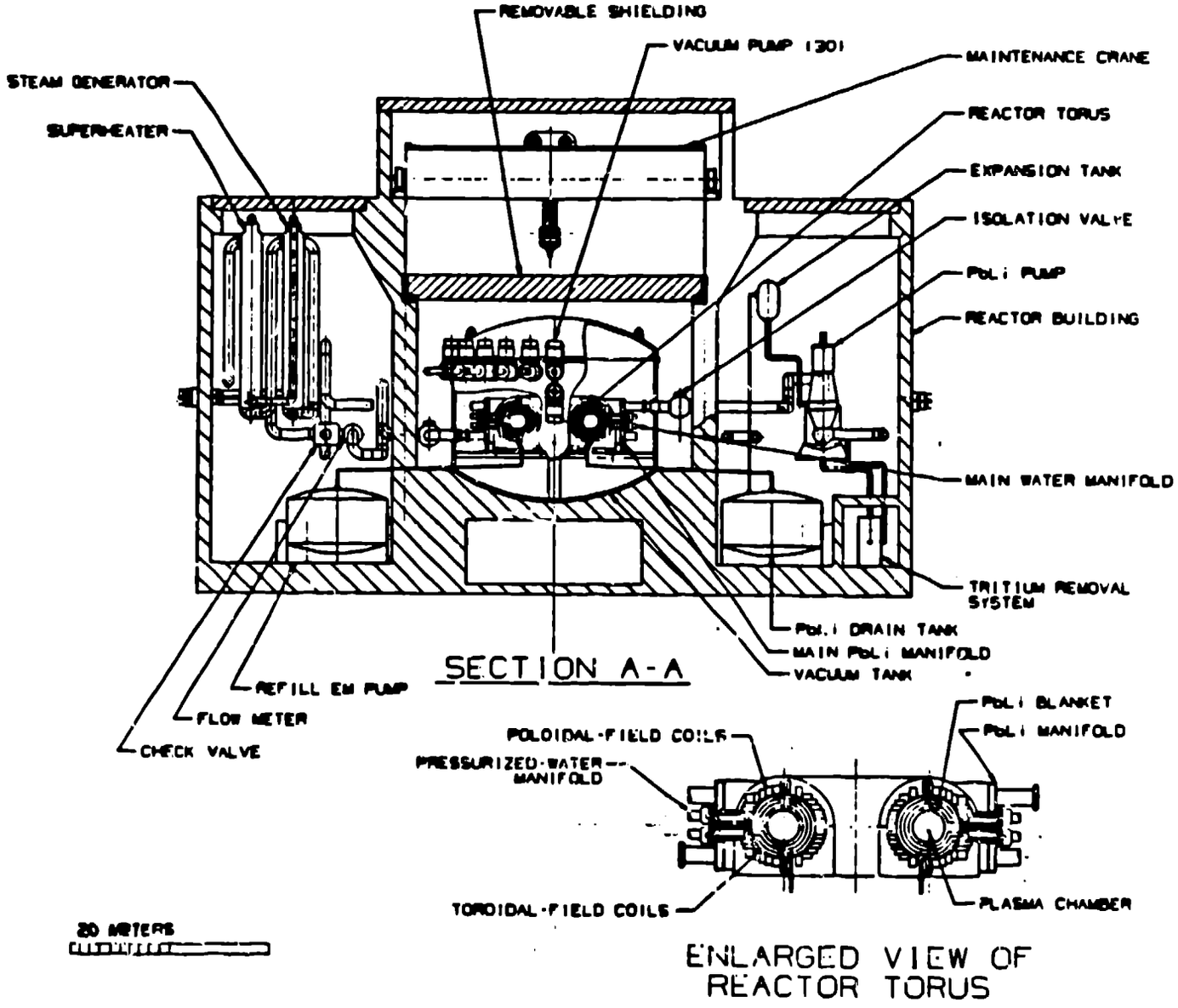

Fig. 10. Reactor plant layout adopted for vertical removal of the FPC.